2014 IEEE International Conference on Robotics & Automation (ICRA)
Hong Kong Convention and Exhibition Center
May 31 - June 7, 2014. Hong Kong, China

Blind Collision Detection and Obstacle Characterisation Using a Compliant Robotic Arm

Piyamate Wisanuvej, Jindong Liu, Ching-Mei Chen, and Guang-Zhong Yang

Abstract— **This paper presents a novel blind collision detection and material characterisation scheme for a compliant robotic arm. By the incorporation of a simple MEMS accelerometer at each joint, the robot is able to detect collision, identify the material of an obstacle, and create a map of the environment. Detailed hardware design is provided, illustrating its value for building a compact and economical robot platform. The proposed method does not require the additional use of vision sensor for mapping the environment, and hence is termed as 'blind' collision detection and environment mapping. Based on the shock wave and vibration signals, the proposed algorithm is able to classify a range of materials encountered. Detailed laboratory evaluation was performed with controlled obstacle collision from different orientation and locations with varying force and materials. The proposed method has achieved 98% detection sensitivity while maintaining 77% specificity. Furthermore, by using sound feature extraction and machine learning techniques, the classifier produces an accuracy of 98% for classifying four different impact materials. In this paper, we also demonstrate its use for detailed environment mapping by using the proposed method.**

I. Introduction

Research in compliant robots working safely in human environment is an increasingly popular research topic because of the wide range of applications under development. These cover human-robot cooperation, learning-from-demonstration, and rehabilitation and healthcare applications. The robot designed to work with human interaction must be able to operate safely and cause no harm to human or damage to properties. In particular, avoiding collision is one of the crucial components for safe robot operation. Typically, this requires vision- or laser-based perception systems. Occlusion in the field of view or very fast movement can cause visual based collision avoidance to fail. The use of integrated sensors for collision detection has many advantages, which can also complement the commonly used vision sensor to improve the overall sensitivity and robustness of the robot.

Thus far, extensive research has been carried out for equipping a robot manipulator with low-level sensors to ensure safe operation. By observing joint position and commanded joint torque, collision detection can be achieved without additional sensor [1], [2], [3]. However, this requires calculations of robot dynamics. Therefore, the method requires complex structural analysis of the robotic arm. Another detection system based on current sensing eliminates the needs of structural analysis and dynamics calculations [4]. However, the method still suffers from the drawback that it only works when the arm is moving and there is no sense of localisation of the collision point.

An alternative method achieves collision detection in quadruped mobile robot by using an accelerometer to monitor the robot movement [5]. The statistical analysis of the signal in frequency domain enables the collision events to be detected. However, location, magnitude, and direction information of the impact are not detected.

In addition to the collision detection, being able to identify obstacle characteristics is also important in practice. The robot controller can store the object location as a static obstacle and navigate around it in subsequent motion planning. On the other hand, collision with human could be considered as dynamic obstacle. Robot may temporarily remember the collision point and avoid that with a certain safety distance.

We all know that humans can sense the hardness of an object by tapping [6]. In the same way, research in object identification also relied on tapping with robotic arm/hand with the obstacles. By capturing the vibration signal with an accelerometer, tapping different objects can produce different vibration patterns [7], [8], [9], [10]. As an example, a legged robot has been proposed, which can identify its walking surface from accelerometer data analysis with machine learning [11]. Despite its high accuracy in surface prediction, this method is based on a walking robot. The signal pattern is different from tapping signal, and thus cannot be used directly to perform object recognition. In addition to tactile sensing, other sensory feedback can also be used. By analysing contact sound from robotic manipulator, the object material can also be identified [12], [13], [14]. Furthermore, object identification can be achieved by characterising its thermal property using robotic manipulator with heat/thermal sensors [15].

By attaching sensors onto the robotic manipulators, environment exploration can be realised. Although contactless approaches using laser range scanner [16] or time-of-flight camera [17] are commonly used, they require complex hardware/software integration. Currently, some approaches using tactile based sensor are being proposed. For example, a robot hand with 256-point piezoresistive sensor array can provide high spatial resolution for contact object identification [18]. Another method is to use a robotic arm with optical waveguide tactile sensor to identify characteristic features on test objects [19].

MEMS accelerometers are commonly used in aforementioned methods because of its compact size, low cost, high bandwidth and high sensitivity. This paper proposes an

Piyamate Wisanuvej, Jindong Liu, Ching-Mei Chen, and Guang-Zhong Yang are with the Hamlyn Centre for Robotic Surgery, Imperial College London, UK. {piyamate.w12, j.liu}@imperial.ac.uk

Materials presented in this paper are part of the completed Master's thesis at The Hamlyn Centre for Robotic Surgery, Imperial College London

978-1-4799-3684-7/14/$31.00 ©2014 IEEE

approach by using MEMS accelerometers integrated with the robotic manipulator for:

1) Collision detection, impact location, direction, and magnitude estimation
2) Material property (hardness) identification
3) Unknown environment exploration and mapping

In this work, we modified an off-the-shelf robotic arm by rebuilding all the control electronics. By adding current sensor as a means of torque sensing, the arm becomes compliant with a torque controller. The accelerometer on board is used to capture the contact vibration of this compliant arm. By processing the acceleration data, the arm can detect the collision and estimates its location, direction, and magnitude. Additionally, the signal is processed further by using machine-learning algorithms to identify the material characteristics of the object. Finally, a blind exploration technique is implemented by using the proposed collision detection method.

II. Methodology

This section describes the implementation of the robotic arm. Details on hardware construction are presented along with the software implementation considerations for solving the blind collision detection, material identification, and exploration problems.

A. Robot Hardware

A 7 degree-of-freedom robotic arm *Cyton Alpha 7D 1G* (Robai, Philadelphia, PA) is used as the basis of our robot design, but with several major modifications. This is shown in Fig. 1. Originally, each joint of the robot is equipped with a hobby servo motor. The improved version of the electronic boards for the motors are built to accommodate the required sensors including the current sensor, accelerometer, and magnetic encoder. The motor is driven by PID controllers with current and position control loops. The motor current is limited at a preset level to provide compliant control. The complete electronics is fitted inside each joint of the robot as shown in Fig. 2. The 3-axis accelerometer (Analog Devices ADXL346) is configured for ± 16g measurement range and 3200 Hz data rate.

B. Blind Collision Detection

Accelerometers inside the robot joints give detailed readings of acceleration from each joint. In normal operating condition, the only source of acceleration signal is from the arm movement itself. This acceleration due to movement usually has a low frequency less than 100 Hz. In case of collision events, external force applied to the arm affects the acceleration significantly. The sudden impact with an external object causes vibration with much higher frequencies. Fig. 3 shows the acceleration signal due to arm movement with collisions. An example of high frequency vibration from the impact is shown in Fig. 4, the parameters are explained in the following.

1) Detection: Due to the large difference in signal patterns from movement and collision signals, the peak pulse from collision can be easily detected using two criteria: Magnitude Threshold Tm and Time Threshold Tt. The time window is a threshold to accept only short peaks. This effectively filters out the acceleration peak from jittery robot movement causing false positives. The magnitude threshold is for filtering out the low joint vibration from the motor and gear system themselves.

Since each robot joint has its own sensor, a total of 9 acceleration readings are obtained in real-time. This provides redundancy in the system, as each part of the arm is being monitored. By having sensors on different parts throughout the robot, the collision events can also be localised. When a collision occurs, the vibration propagates from the point of impact through the links and joints that connect together.

Consider the case of a collision occurred in the i^{th} link, the circuit board and sensor is rigidly connected to the i^{th} joint casing and i^{th} link. Whereas the $i+1^{th}$ and $i-1^{th}$ link connect to the output shaft through the gearing system. The vibration propagation via rigid connection loses less energy than loose connection. The reduction gearing in the robot joint has around 4-5 stages with the ratio in ranges of 1:30-1:500. This causes the vibration magnitude to be greatly decreased because of the reduced torque when transferred through the gearing system, effectively damping the vibration signal propagation. With this simplified model, it suggests that the joint closest to the impact gets the highest signal. Thus, by comparing the signal magnitude the link-level localisation can be achieved. The magnitudes of the signal $(A_k : A_x, A_y, A_z)$ are obtained from the peak amplitude of the collision signal.

$$m = \sqrt{A_x^2 + A_y^2 + A_z^2} \tag{1}$$

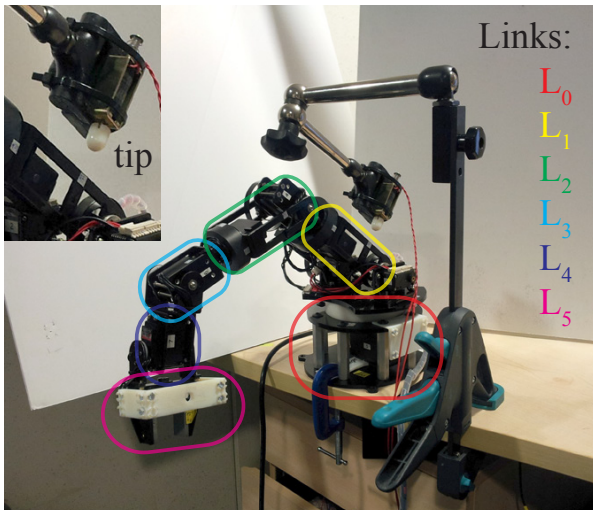

Fig. 1: The experiment setup of a robotic arm and a solenoid with interchangeable hardness tips (showing the white tip in enlarged image). The arm is divided into 6 links (L0- L5) for the purpose of location identification of collisions.

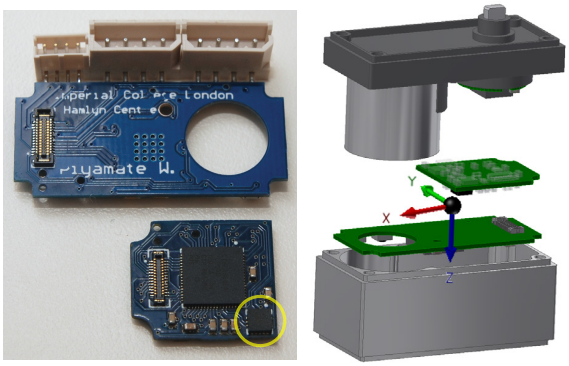

(a) Printed circuit boards (b) Circuit assembly

Fig. 2: The circuit board assembly of the customised servo motor for the robotic arm. The yellow circle indicates the location of the accelerometer. The axes illustrate the alignment of the sensor's coordinate frame.

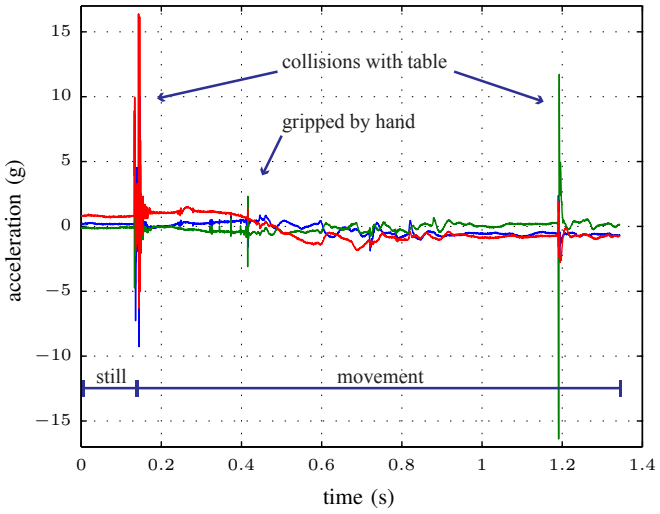

Fig. 3: Acceleration signals of the arm's end effector showing hard collisions (with wooden table) and general collision (with finger) along with an arm movement

2) Direction and magnitude estimation: Each accelerometer sensor has 3 axes, arranged in XYZ Cartesian coordinates. This gives directional information of the collision. Since the sensor provides Cartesian output format, the absolute magnitude m of the signal can be calculated by Root Mean Square value. Additionally, the impact direction can be obtained by the coordinate transformations of the sensor's coordinate frame inside the joint to the global reference frame.

It is important to note that the accelerometer signal contains earth's gravitational acceleration component. This measurement should be subtracted because it affects the calculation by shifting the whole signal with this offset. From the sensor's point of view, this Baseline Acceleration B_i changes according to the orientation of the sensor relative to the ground, including its movement. This can be determined from the kinematics calculation. A simpler approach can also

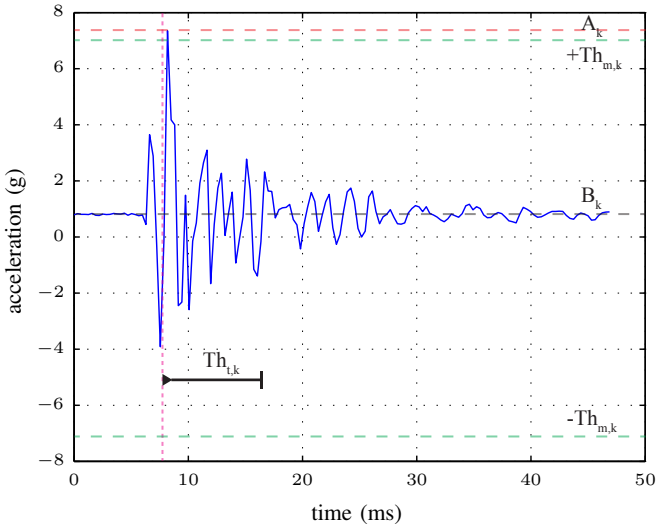

Fig. 4: Parameters of a collision signal in k^{th} axis: Magnitude A_k, Baseline Acceleration B_k, Amplitude Threshold $\pm Tm_k$, and Time Threshold Tt_k

be used. Since the vibration from any impact is typically very short (less than 20 milliseconds) compared to the change of acceleration from the arm movement, the baseline gravitational acceleration can be determine temporarily in each collision event. This signal baseline can then be obtained by calculating the median of the signal, which takes into account the sensor's offset as well.

The direction of impact in sensor's frame can be represented by Euler's angles (θ, ϕ, ψ). These angles are obtained from acceleration magnitudes using these equations derived in [20].

$$\theta = \arctan\left(\frac{A_x}{\sqrt{A_y^2 + A_z^2}}\right) \tag{2a}$$

$$\phi = \arctan\left(\frac{A_y}{\sqrt{A_x^2 + A_z^2}}\right) \tag{2b}$$

$$\psi = \arctan\left(\frac{\sqrt{A_x^2 + A_y^2}}{A_z}\right) \tag{2c}$$

C. Object Identification

When different materials hit an object, varying sound signatures are produced. Human can roughly identify the material by the impact sound ourselves. This suggests that impact vibration caused by collision has its own characteristics based on the material. Since the acceleration from impact vibration follows a similar pattern as in impact sound [21], similar techniques of sound processing can be used. Sample signal from collision with different materials are shown in Fig. 5. The vibration signal can be processed using the machine learning techniques. Using the previous detection method, the collision signal can be segmented. By considering the vibration signal as a sound, its characteristics can be

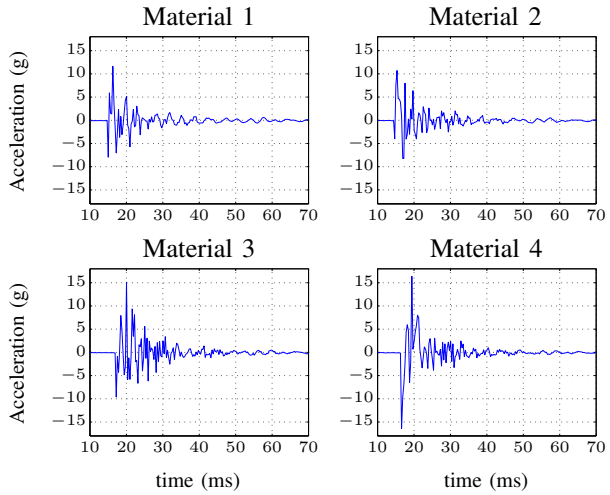

Fig. 5: Acceleration signals for collisions from different materials used in experiments

described by comprehensive amount of sound features. These features can be extracted by sound processing software. Then classifiers are used to build a model of material classification based on the vibration features.

In order to process the signal with the classifiers, its features need to be extracted. As the vibration signal is a time-domain signal similar to the voice signal (with lower frequency), the audio features extraction library is used to obtain those features. The *YAAFE – Yet Another Audio Feature Extractor* [22] is used. The list of features used are shown in Table II.

The classifiers used are the following: J48 Decision Tree, SVM, Neural Network (Multilayer Perceptron), Linear Regression, and Naive Bayes.

D. Environment Exploration

As the manipulator has capability of collision detection, this can be extended further to perform blind exploration (without visual sensors). With the known robot kinematics, each joint location in space can be calculated. When the robot hits an unknown obstacle within the environment, its position based on location of impact can be determined. By simultaneously moving the robot around in space to collect collision data, the point cloud of the environment can be created. With the information of impact direction, each collision point is tagged with a normal vector. The plane can be estimated with this vector to build a surface mesh of the environment.

III. Experiments

To evaluate the accuracy of each of the proposed methodologies, detailed laboratory experiments have been performed. The experiments conducted contain three parts. In the first two experiments, arm is configured to be stationary, whereas the arm is manually controlled in the third experiment.

A. Collision Detection

The experiment is carried out as shown in Fig. 1. A solenoid is used as a tool to hit the robotic arm in different locations. It is rigidly fixed to the table with a clamp. The tip of the solenoid is a round shaped rigid plastic. In each hit, the experiment is configured with three variables: link number, direction, hit magnitude. The robot has six links. Each link is hit with two directions perpendicular to the link's surface. Each combination of location and direction is hit with three different magnitudes and repeat for 10 times. This experiment format collected a total of 360 collisions.

B. Object Identification

The experiment is setup in a similar way as previous. The only difference is that the tip of the solenoid is also a controlled variable. Four different tips are built from a 3D printer using different materials. We call these material M_1, M_2, M_3, M_4. The material properties are shown in Table I. All tips have identical shape.

Mat.	Tensile strength(MPa)	Shore hardness	Elongation at break (%)	Equivalent Material
1	0.8-1.5	26-28 (A)	170-220	Rubber band
2	2-4	55-65 (A)	80-100	Eraser
3	15-25	90-100 (A)	25-35	Tyre
4	50-65	83-86 (D)	10-25	Plastic helmet

TABLE I: Material properties of the solenoid tips used in the object identification experiment

In this experiment, each object hits the robotic arm repeatedly 100 times on the same spot. Together with 12 possible combinations of variables, the total number of datasets are 1200. Each material is considered as a class, hence there are total of 4 classes with 300 datasets for each class.

With extracted features, the total number of attributes for each dataset is 397. All datasets are fed into 5 classifiers to perform the classification. The dataset is split into 90% training set and 10% testing set. The data splitting is performed using the cross-validation method so the splitting is randomised and distributed equally. The classification is done using *Weka – Waikato Environment for Knowledge Analysis* software [23]. The parameters used in the classifiers are default values supplied by the software.

C. Environment Exploration

For environment exploration, the experiment setup includes two scenarios. For the first scenario, the rectangular box is placed to cover the arm workspace. Additional sloped plastic plate is added as another obstacle for the second scenario. The flat surface is chosen for the simplicity for data collection and result evaluation. To simplify the arm trajectory generation, the arm is controlled manually by a human operator. A Phantom Omni (Sensable, Wilmington, MA) haptic device is used as a controller. It has 6 degrees of freedom. All of the degrees of freedom are mapped to the joint angle of the robotic arm. Scaling is applied to make the operating range of the haptic device matches the joint range

(a) Scenario 1 (b) Scenario 2

Fig. 6: Experiment setups of environment exploration, Scenario 1: arm in an empty box, Scenario 2: an obstacle is added into the box

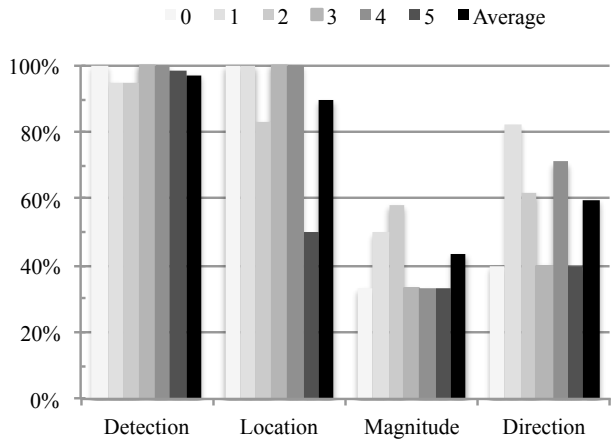

Fig. 7: Collision detection and estimations accuracy for each robot's link corresponding to Fig. 1

of the robot. Since the arm has an extra degree of freedom, compared to the controller, one of the arm's joint is kept stationary.

The translucent plastic box is used. The inside dimension of the box is $62.7 \times 39 \times 35.3$ cm. Obstacle in the first scenario is the box itself. Due to workspace constrain, only 4 of the sides are reachable. The second scenario involves one sloped plane as an obstacle in addition to the box. This makes the second scenario have 5 reachable sides. The data collection is performed by capturing the joint angles and the acceleration signal at the same time. The movement of the robotic arm is determined by user's decision, with best effort to reach as many faces of the obstacle as possible. Fig. 6 shows the experiment setup in two scenarios.

IV. Results

A. Collision Detection

The experiment evaluations can be divided into 4 parts: *Collision Detection, Collided Link Location Identification, Magnitude Estimation, and Direction Estimation*. These experimental results are shown in Fig. 7. Regarding the *Collision Detection*, the sensitivity of 98% and specificity of 77% are achieved.

B. Object Identification

Fig. 8 shows a comparison of the classification accuracy. Three of them give very accurate results, with the highest of

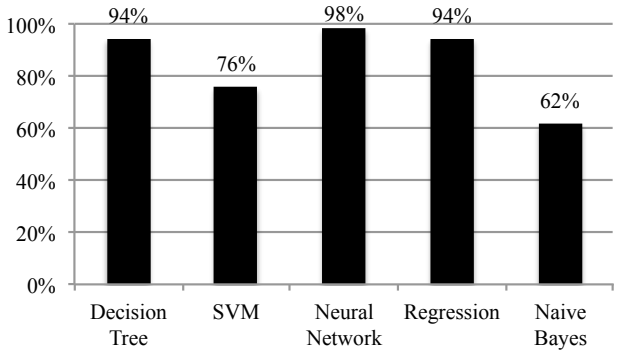

Fig. 8: Object identification accuracy

Ranking	Feature
0.92	Auto Correlation
0.91	Energy
0.84	Temporal Shape Statistics
0.79	f_p
0.68	Spectral Shape Statistics
0.51	Envelope Shape Statistics
0.50	Zero Crossing Rate
0.32	t_p
0.23	Spectral Rolloff

TABLE II: *InfoGain* ranking values for the signal features used, higher values mean higher contribution to classification accuracy

98%. With further analysis from the attribute selection tool in Weka, it is shown that some of the features contribute a major part of the accurate result, and some are not contributing at all. By using Ranker attribute selection, the result shown in Table II is the list of ranking value sorted by *InfoGain* evaluation [23]. This gives a rough clue of which features contribute most to the classification accuracy.

C. Environment Exploration

Captured data points from two scenarios are shown in Fig. 9. It also shows the superimposed location of the actual obstacle surface. Both scenarios have approximately 160 collision points. Each colour of the points represents each surface of the learned environment. The Root Mean Square Error of the collected data compared to the nearest obstacle's surface are 26.7mm and 14.9 mm for the first and second scenario respectively.

V. Conclusions

In this paper we have presented a blind approach of collision detection for a robotic arm using accelerometer. The result shows that the proposed method has accurate detection while maintaining a reasonable specificity level. The impact location can be also determined in terms of collided link, with a considerable accuracy. However, the estimation of impact direction and magnitude are not yet satisfying. This deserves further investigation. We believe that the mechanical configuration of robot makes the vibration signal distorted.

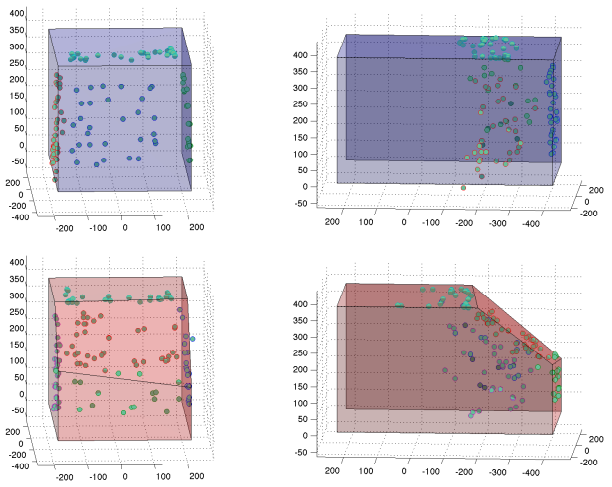

(a) Front (b) Side

Fig. 9: Exploration results, top plots show the 1st scenario, bottom plots show the 2nd scenario, axes are in millimetres

Therefore, the magnitude and direction calculations (Equations 1 and 2) can become problematic.

Another possible improvement to the blind collision detection problem is to localise the impact within the link. Since the vibration signal is a wave that propagates through the link material, collisions at different locations make the signals arrive the sensors on both sides at different times. We can possibly use time difference of arrival (TDOA) technique to implement the localisation [24].

The accuracy of the experimental results in terms of object identification proves that accelerometer has very high potential to capture the difference in vibration patterns from different materials. In this experiment, only 4 prototype materials have been used. This should be improved by adding more material in everyday life to prove this approach in the practical level.

The result from preliminary work on blind environment exploration method is promising. This demonstrates one possible application of using simple accelerometer to implement a blind robot perception system. The current method are only limited to collecting point cloud of the environment since the impact direction estimation is not accurate. If this estimation could be improved, however, the normal vector of each point would be available. Therefore, instead of collecting points, planes would be collected. This could be merged into three dimensional mesh and provide more realistic reconstruction of the environment.

REFERENCES

[1] A. D. Luca and R. Mattone, "Sensorless Robot Collision Detection and Hybrid Force / Motion Control," in *IEEE International Conference on Robotics and Automation (ICRA)*, no. April, 2005, pp. 999–1004.

[2] A. Luca, A. Albu-Schaffer, S. Haddadin, and G. Hirzinger, "Collision Detection and Safe Reaction with the DLR-III Lightweight Manipulator Arm," in *IEEE/RSJ International Conference on Intelligent Robots and Systems (IROS)*. Ieee, Oct. 2006, pp. 1623–1630.

[3] S. Haddadin, A. Albu-Schaffer, A. De Luca, and G. Hirzinger, "Collision detection and reaction: A contribution to safe physical human-robot interaction," in *IEEE/RSJ International Conference on Intelligent Robots and Systems (IROS)*, 2008, pp. 22–26.

[4] H.-W. Je, J.-Y. Baek, and M. C. Lee, "Current based compliance control method for minimizing an impact force at collision of service robot arm," *International Journal of Precision Engineering and Manufacturing*, vol. 12, no. 2, pp. 251–258, Apr. 2011.

[5] T. Meriçli, c. Meriçli, and H. Akn, "A robust statistical collision detection framework for quadruped robots," *RoboCup 2008: Robot Soccer World Cup XII*, 2009.

[6] R. H. Lamotte, "Softness Discrimination With a Tool," *Journal of Neurophysiology*, vol. 83, no. 4, pp. 1777–1786, 2013.

[7] K. Kuchenbecker, J. Fiene, and G. Niemeyer, "Event-Based Haptics and Acceleration Matching: Portraying and Assessing the Realism of Contact," *First Joint Eurohaptics Conference and Symposium on Haptic Interfaces for Virtual Environment and Teleoperator Systems*, pp. 381–387, 2005.

[8] J. Romano and K. Kuchenbecker, "Creating realistic virtual textures from contact acceleration data," *Haptics, IEEE Transactions on*, vol. 5, no. 2, pp. 109–119, 2012.

[9] J. Windau, "An Inertia-Based Surface Identification System," in *2010 IEEE International Conference on Robotics and Automation*. Ieee, May 2010, pp. 2330–2335.

[10] H. Liu, X. Song, and T. Nanayakkara, "Friction estimation based object surface classification for intelligent manipulation," in *IEEE ICRA 2011 workshop on autonomous grasping, Shanghai*, 2011.

[11] D. Vail and M. Veloso, "Learning from Accelerometer Data on a Legged Robot," in *5th IFAC/EURON Symposium on Intelligent Autonomous Vehicles*, 2004.

[12] E. Torres-jara, L. Natale, and P. Fitzpatrick, "Tapping into Touch," in *Fifth International Workshop on Epigenetic Robotics: Modeling Cognitive Development in Robotic Systems*, 2005, pp. 79–86.

[13] J. Richmond and D. Pai, "Active Measurement of Contact Sounds," in *Robotics and Automation, 2000. Proceedings. ICRA'00. IEEE International Conference on*, vol. 3, 2000, pp. 2146–2152.

[14] S. Femmam, "Perception and characterization of materials using signal processing techniques," *Instrumentation and Measurement, IEEE Transactions on*, vol. 50, no. 5, pp. 1203–1211, 2001.

[15] M. Campos, R. Bajcsy, and V. Kumar, "Exploratory procedures for material properties: The temperature perception," in *Advanced Robotics, 1991.'Robots in Unstructured Environments', 91 ICAR., Fifth International Conference on*, 1991.

[16] G. Paul, D. K. Liu, N. Kirchner, and S. Webb, "Safe and Efficient Autonomous Exploration Technique for 3D Mapping of a Complex Bridge Maintenance Environment," in *24th International Symposium on Automation and Robotics in Construction (ISARC 2007)*, 2007.

[17] T. Kunz, U. Reiser, M. Stilman, and A. Verl, "Real-time path planning for a robot arm in changing environments," in *2010 IEEE/RSJ International Conference on Intelligent Robots and Systems*. Ieee, Oct. 2010, pp. 5906–5911.

[18] P. Allen and P. Michelman, "Acquisition and interpretation of 3-D sensor data from touch," *IEEE Transactions on Robotics and Automation*, vol. 6, no. 4, pp. 397–404, 1990.

[19] A. M. Okamura, "Feature Detection for Haptic Exploration with Robotic Fingers," *The International Journal of Robotics Research*, vol. 20, no. 12, pp. 925–938, Dec. 2001.

[20] M. Pedley and Freescale Semiconductor, "AN3461: Tilt Sensing Using a Three-Axis Accelerometer," 2013.

[21] W. McMahan, E. D. Gomez, L. Chen, K. Bark, J. C. Nappo, E. I. Koch, D. I. Lee, K. R. Dumon, N. N. Williams, and K. J. Kuchenbecker, "A practical system for recording instrument interactions during live robotic surgery," *Journal of Robotic Surgery*, Apr. 2013.

[22] B. Mathieu, S. Essid, T. Fillon, J. Prado, and G. Richard, "YAAFE, an Easy to Use and Efficient Audio Feature Extraction Software," in *ISMIR*, no. Ismir, 2010, pp. 441–446.

[23] M. Hall, E. Frank, and G. Holmes, "The WEKA data mining software: an update," *ACM SIGKDD Explorations Newsletter*, vol. 11, no. 1, pp. 10–18, 2009.

[24] K. R. Arun, E. Ong, and A. W. H. Khong, "Source localization on solids using Kullback-Leibler Discrimination Information," *International Conference on Information, Communications and Signal Processing (ICICS)*, pp. 1–5, Dec. 2011.